Four-Pulse ELDOR Theory of the Spin ½ Label Pairs Extended to Overlapping EPR Spectra and to Overlapping Pump and Observer Excitation Bands

K. M. Salikhov · I. T. Khairuzhdinov

Abstract The current theory of the four-pulse electron double resonance (PEL-DOR) has been extended to take into account two effects: (1) overlapping of the electron paramagnetic resonance (EPR) spectra of paramagnetic spin ½ particles (spin labels) in pairs and (2) overlapping of the excitation bands by the pump and echo-forming pulses. It has been shown that the PELDOR signal contains additional terms in contrast to the situation considered in the current theory, when the EPR spectra of the spin labels in the pairs and the excitation bands do not overlap. All terms oscillate with the same frequency, which is the characteristic dipolar interaction frequency. The largest additional terms originate from the fact that both spins in pairs can be excited by the echo-forming pulses when the EPR spectra of the partners in pairs overlap essentially. The results of the numerical calculations, which illustrate the possible scale of the effect of these additional terms on the PELDOR signal, are presented.

1 Introduction

The relatively small spin–spin interaction between paramagnetic centers in solids can be detected by observing the behavior of the electron spin echo (ESE) signals [1–3]. Among the most popular protocols of the ESE experiments are the two-pulse echo, which is known as the Hahn echo or the primary echo, and the three-pulse echo experiments. The "2 + 1" pulse train electron spin resonance method was suggested in Refs. [4, 5]. For these protocols, the exchange and dipole–dipole interactions between partners in pairs of the paramagnetic particles can cause the modulation of the ESE signals [6]. However, this modulation of the echo signal

K. M. Salikhov (✉) · I. T. Khairuzhdinov
Zavoisky Physical-Technical Institute, Russian Academy of Sciences,
Sibirsky trakt 10/7, 420029 Kazan, Russian Federation
e-mail: salikhov@kfti.knc.ru

decay is manifested only when the microwave (MW) pulses excite both partner spins in pairs. This happens, e.g., when both partners in pairs are identical (like) paramagnetic particles. When partners in pairs are not identical paramagnetic particles, only one partner spin in pairs can be excited by the MW pulses, which form the echo signal. In this situation, the spin–spin interaction between two partner spins in pairs is not manifested as the modulation effect of the echo signal decay unless this spin–spin interaction is randomly modulated by the spin–lattice relaxation and/or the molecular motion [7, 8]. To extend the application of the ESE methods for measuring the spin–spin interaction between unlike spins, it was proposed to use the pulse electron double resonance (PELDOR) protocol [9]. In Ref. [9], the three-pulse ELDOR experiment was proposed as a modification of the primary echo protocol by adding the MW pulse field with the frequency that differs from the frequency of the echo-forming MW pulses. Thus, the primary echo signal modulation effect is induced by applying an additional MW pulse due to the spin–spin interaction between unlike partner spins in pairs. The physical background of using the PELDOR effect to determine the distance between two paramagnetic particles in the range of 1–8 nm was comprehensively discussed in a number of publications (see, e.g., [10–14]). The theory of the three-pulse ELDOR was comprehensively discussed also recently in Ref. [15].

Another protocol of the dead-time-free four-pulse ELDOR experiment was presented in Refs. [16–18] (see Fig. 1).

In this case, three MW pulses at $t = 0$, $t = \tau_1$, $t = 2\tau_1 + \tau_2$ with the frequency ω_A induce several echo signals, one of them arises at $t = 2\tau_1 + 2\tau_2$ (see Fig. 1). The spin–spin interaction between paramagnetic particles in pairs is manifested as the modulation of the echo signal decay curve for the echo signal observed at $t = 2\tau_1 + 2\tau_2$ (see below). By adding the fourth MW pulse at $t = \tau_1 + T$ with the frequency ω_B, one can highlight this modulation effect, i.e., observe oscillations of the signal as a function of the time interval T.

The current theory of this four-pulse ELDOR is developed for the case when the EPR spectra of the partner spins in the pair do not overlap so that the MW pulses
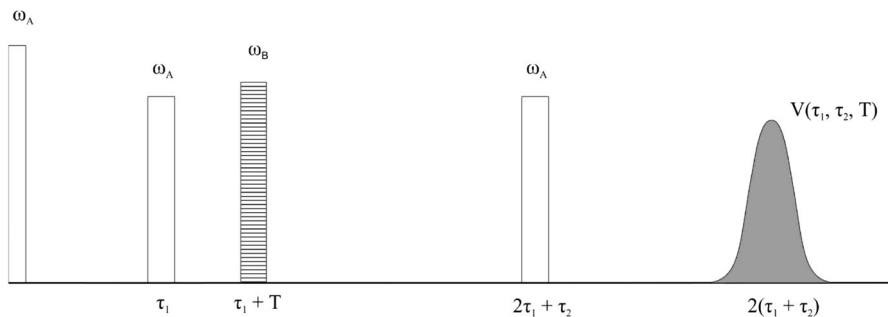

Fig. 1 Protocol of the four-pulse ELDOR experiment [16]. The spin echo is formed by the excitation MW pulses with the frequency ω_A at $t = 0$, $t = \tau_1$ and $t = 2\tau_1 + \tau_2$. The additional (pump) MW pulse with the frequency ω_B at $t = \tau_1 + T$ affects the spin echo signal. Durations of pulses at $t = 0$, τ_1, $\tau_1 + T$, and $2\tau_1 + \tau_2$ are t_{p1}, t_{p2}, t_{p3} and t_{p4}, respectively

with frequencies ω_A and ω_B excite different partner spins in the pair, and the probability that any spin in the pair can be noticeably excited by the MW pulses of both frequencies is supposed to be negligible [16–18]. In the case of the spin label pairs, which have overlapping EPR spectra, new options appear: both partner spins in the pair can be excited by echo-forming and/or pump MW pulses. This possibility was not considered in detail in the current PELDOR theory although it was qualitatively understood that in the presence of overlapping of the EPR spectra, there is a way of excitation when both partners are excited by the echo-forming pulses (see, e.g., [19]).

For the further discussion let us consider the AB pairs. Suppose that the A spins are excited only by the three echo-forming MW pulses with the frequency ω_A, while the B spins are excited efficiently only by the additional fourth MW pulse with the frequency ω_B. In this model situation, the contribution of the dipole–dipole interaction inside the AB pair to the four-pulse ELDOR signal under consideration is presented as [16–18].

$$V(T, \tau_1, \tau_2) = 1 - p_B + p_B \cos(D_{AB}(T - \tau_1)), \tag{1}$$

where p_B is the probability of the inversion of the spins B by the pump MW pulse at $t = \tau_1 + T$, and D is the parameter of the dipole–dipole interaction.

$$H_{d-d} = \hbar D_{AB} S_{Az} S_{Bz}, \tag{2}$$

$$D_{AB} = \frac{g_A g_B \beta^2}{\hbar r_{AB}^3} \left(1 - 3\cos^2\theta\right) \equiv D_{0AB}\left(1 - 3\cos^2\theta\right) \tag{3}$$

Here, r_{AB} is the distance between spins A and B, θ is the angle between the vector r_{AB} and the direction of the external magnetic field. Here, we assume that the g-tensors of spin labels are isotropic. We suppose that the distance between the partner spins in the pair is larger than 1 nm so that the contribution of the short-range Heisenberg exchange interaction between particles can be ignored (the range of distances preferable for PELDOR was discussed in [20, 21]. Possible effects of the exchange interaction on the PELDOR signal were discussed in [20–24].

In real systems, e.g., nitroxides, the spin Hamiltonians of the Zeeman interaction, nitrogen hyperfine, and electron spin–spin interactions have isotropic and anisotropic contributions. As a result, the EPR frequencies depend on the spatial orientation of paramagnetic centers. These anisotropic effects should be taken into account when calculating the EPR spectrum shape and the probability of the inversion of spins by MW pulses. The orientation selectivity effects were discussed in numerous publications (see, e.g., [19, 25–28]). In this paper, we do not focus on these orientation selectivity effects. Our goal is to highlight effects which are induced by overlapping of the EPR spectra of partners and possible overlapping of the excitation bands of the pulses used in the four-pulse ELDOR experiments.

Equation (1) was derived for the situation, when partners in the pair are paramagnetic particles with the EPR spectra, which do not overlap, so that these partners can be excited selectively by MW pulses. At present Eq. (1) is also used for interpreting the PELDOR data in the cases, when the particles in pairs are nitroxide-free radicals with overlapping or coinciding EPR spectra. Therefore, it is necessary

to study whether Eq. (1) is applicable to the systems, when both spin labels in pairs are paramagnetic particles with close magnetic resonance parameters, so that their EPR spectra overlap substantially.

In this work, we generalize Eq. (1) and derive the contribution of the intra-pair interaction to the four-pulse ELDOR signal, when the EPR spectra of the partner spin labels in the pair overlap (or even coincide). It appears that the PELDOR signal contains additional terms in contrast to the situation considered in the current theory, when the EPR spectra of the spin labels in the pairs do not overlap. These new terms arise as a result of the possible excitation of both spins in the pair by the MW pulses with the frequency ω_A and of the possible excitation of the same spin by both ω_A and ω_B frequencies MW pulses used during the PELDOR experiments.

2 Theoretical Considerations

In this work, we use the model analogous to that used in our previous work [15] where we have comprehensively discussed the three-pulse ELDOR theory. Therefore, we will not describe the model in detail. Instead, we will present it here only shortly. Detail description can be found in Ref. [15].

We consider an ensemble of pairs of paramagnetic particles (spin labels) R_1 and R_2 with the electron spins ½, when their EPR spectra $g_1(\omega)$ and $g_2(\omega)$ overlap. Let us assume that the spin echo-forming MW pulses have the frequency ω_A and the pump MW pulse has the frequency ω_B. In the PELDOR experiments, the MW pulses with frequencies ω_A and ω_B excite spins with the resonance frequencies in intervals $(\omega_A - \omega_{1A}, \omega_A + \omega_{1A})$ and $(\omega_B - \omega_{1B}, \omega_B + \omega_{1B})$, respectively. Here ω_{1A} and ω_{1B} denote the Rabi frequencies of the MW pulses. We assume that pulses with frequencies ω_A and ω_B can rotate, in principle, the spins of both partners R_k, $k = 1$, 2. We consider systems when the interaction between spins in pairs is relatively small compared to the Rabi frequencies ω_{1A}, ω_{1B}. Under this condition, the probability of the spin inversion is calculated as follows. Let us denote the resonance frequency of the spin R_k as Ω_k and the probability of the reorientation of the spin R_k by the MW pulse, which has duration t_p, the frequency ω_F, and the Rabi frequency ω_{1F} as $p(\Omega_k | \omega_F, t_p)$, $k = 1$, 2, $F = A$, B. Then

$$p\left(\Omega_k | \omega_F, t_p\right) = \frac{\omega_{1F}^2}{\omega_{1F}^2 + (\Omega_k - \omega_F)^2} \sin^2\left[\sqrt{\omega_{1F}^2 + (\Omega_k - \omega_F)^2} \frac{t_p}{2}\right] \qquad (4)$$

Let us divide the ensemble of pairs $R_1 R_2$ into sub-ensembles with the different inversion patterns of spins R_1 and R_2 by the MW pulses at the moments τ_1, $\tau_1 + T$, $2\tau_1 + \tau_2$ during the four-pulse ELDOR experiment (see Fig. 1). In PELDOR experiments, the time intervals τ_1 and τ_2 are kept constant and the signal is detected as a function of the T value, while the T value changes in the interval $0 < T < \tau_1 + \tau_2$ [16, 17]. The sub-ensembles which contribute to the signal observed at $t = 2\tau_1 + 2\tau_2$ and the shapes of the contributions of these sub-ensembles are given in Table 1. First, let us consider the contribution of one of the partners in the pair, e.g., spin R_1, to the PELDOR signal. The first pulse at $t = 0$

Table 1 Inversion patterns of spins R_1 and R_2 by the MW pulses at the moments τ_1, $\tau_1 + T$, $2\tau_1 + \tau_2$, which contribute to the PELDOR signal, and contributions of spins R_1 to the PELDOR signal

No. of the inversion pattern	Pulse at τ_1	Pulse at $\tau_1 + T$	Pulse at $2\tau_1 + \tau_2$	Contribution to the observed signal
1	Only spin R_1 is inverted	Both spins are not inverted	Only spin R_1 is inverted	$\mathbf{P_{1a}}$
2	Both spins are inverted	Both spins are not inverted	Only spin R_1 is inverted	$P_{1b} \cos(D\tau_1)$
3	Only spin R_1 is inverted	Only spin R_2 is inverted	Only spin R_1 is inverted	$\mathbf{P_{1c} \cos(D(\tau_1 - T))}$
4	Both spins are inverted	Only spin R_2 is inverted	Only spin R_1 is inverted	$P_{1d} \cos(DT)$
5	Only spin R_1 is inverted	Both spins are not inverted	Both spins are inverted	$P_{1e} \cos(D\tau_2)$
6	Both spins are inverted	Both spins are not inverted	Both spins are inverted	$P_{1f} \cos(D(\tau_1 + \tau_2))$
7	Only spin R_1 is inverted	Only spin R_2 is inverted	Both spins are inverted	$P_{1g} \cos(D(\tau_1 + \tau_2 - T))$
8	Both spins are inverted	Only spin $R2$ is inverted	Both spins are inverted	$P_{1h} \cos(D(\tau_2 - T))$

rotates the spin R_1 around the x-axis and creates the average spin moment along the y-axis.

$$m1_y(\Omega_1) = -\frac{1}{2} \frac{\omega_{1A}}{\sqrt{\omega_{1A}^2 + (\Omega_1 - \omega_A)^2}} \sin\left[\sqrt{\omega_{1A}^2 + (\Omega_1 - \omega_A)^2} t_{p1}\right] \quad (5)$$

In Table 1 the following notations are introduced:

D is the parameter of the dipole–dipole interaction in the pair R_1R_2 [see Eqs. (2) and (3)],

$$
\begin{aligned}
M_1 &= \langle m_{1y} p(\Omega_1|\omega_A, t_{p2})(1 - p(\Omega_1|\omega_B, t_{p3}))\ p(\Omega_1|\omega_A, t_{p4}) \rangle, \\
P_{1a} &= M_1 \langle (1 - p(\Omega_2|\omega_A, t_{p2}))(1 - p(\Omega_2|\omega_B, t_{p3}))\ (1 - p(\Omega_2|\omega_A, t_{p4})) \rangle, \\
P_{1b} &= M_1 \langle p(\Omega_2|\omega_A, t_{p2})(1 - p(\Omega_2|\omega_B, t_{p3}))\ (1 - p(\Omega_2|\omega_A, t_{p4})) \rangle, \\
P_{1c} &= M_1 \langle (1 - p(\Omega_2|\omega_A, t_{p2}))p(\Omega_2|\omega_B, t_{p3})\ (1 - p(\Omega_2|\omega_A, t_{p4})) \rangle, \\
P_{1d} &= M_1 \langle p(\Omega_2|\omega_A, t_{p2})p(\Omega_2|\omega_B, t_{p3})\ (1 - p(\Omega_2|\omega_A, t_{p4})) \rangle, \qquad (6) \\
P_{1e} &= M_1 \langle (1 - p(\Omega_2|\omega_A, t_{p2}))(1 - p(\Omega_2|\omega_B, t_{p3}))\ p(\Omega_2|\omega_A, t_{p4}) \rangle, \\
P_{1f} &= M_1 \langle p(\Omega_2|\omega_A, t_{p2})(1 - p(\Omega_2|\omega_B, t_{p3}))\ p(\Omega_2|\omega_A, t_{p4}) \rangle, \\
P_{1g} &= M_1 \langle (1 - p(\Omega_2|\omega_A, t_{p2}))p(\Omega_2|\omega_B, t_{p3})\ p(\Omega_2|\omega_A, t_{p4}) \rangle, \\
P_{1h} &= M_1 \langle p(\Omega_2|\omega_A, t_{p2})p(\Omega_2|\omega_B, t_{p3})\ p(\Omega_2|\omega_A, t_{p4}) \rangle
\end{aligned}
$$

The excitation patterns of spins, which do not contribute to the PELDOR signal, are not given in Table 1. The

contribution of the spin R_2 of the pair to the PELDOR signal is given by expressions similar to those given in Table 1 and Eqs. (6) with subscripts 1 and 2

interchanged. The signal observed in the PELDOR experiments is a sum of contributions of spins R_1 and R_2.

The symbol $<\dots>$ means averaging over the distributions of the EPR frequencies, which are given by the EPR spectra $g_1(\Omega_1)$ and $g_2(\Omega_2)$ of spins R_1 and R_2,

$$\langle f_1(\Omega_1) f_2(\Omega_2) \rangle = \langle f_1(\Omega_1) \rangle \langle f_2(\Omega_2) \rangle = \int f_1(\Omega_1) g_1(\Omega_1) d\Omega_1 \int f_2(\Omega_2) g_2(\Omega_2) d\Omega_2. \tag{7}$$

Thus, the contribution of the spin R_1 to the four-pulse ELDOR signal is

$$\begin{aligned} V_1(T, \tau_1, \tau_2) = \boldsymbol{P_{1a}} &+ \boldsymbol{P_{1b}}\cos(D\tau_1) + \boldsymbol{P_{1c}}\boldsymbol{\cos(D(\tau_1 - T))} + P_{1d}\cos(DT) \\ &+ P_{1e}\cos(D\tau_2) + P_{1f}\cos(D(\tau_1 + \tau_2)) + P_{1g}\cos(D(\tau_1 + \tau_2 - T)) \\ &+ P_{1h}\cos(D(\tau_2 - T)) \end{aligned} \tag{8}$$

Bold font indicates the terms present in the current PELDOR theory. For comparison, we present the echo signal in the absence of the pumping MW pulse. By assuming that $p(\Omega_2|\omega_B, t_{p3}) = 0$, one obtains from Eqs. (6) and (8) that this signal is given by

$$V_{01}(\tau_1, \tau_2) = \boldsymbol{P_{01a}} + P_{01b} \cos(D\tau_1) + P_{01e} \cos(D\tau_2) + P_{01f} \cos(D(\tau_1 + \tau_2)), \quad (9)$$

where

$$\begin{aligned} M_{01} &= \langle m_{1y} p(\Omega_1|\omega_A, t_{p2}) \ p(\Omega_1|\omega_A, t_{p4}) \rangle, \\ P_{01a} &= M_{01}\langle (1 - p(\Omega_2|\omega_A, t_{p2})) \ (1 - p(\Omega_2|\omega_A, t_{p4})) \rangle, \\ P_{01b} &= M_{01}\langle p(\Omega_2|\omega_A, t_{p2}) \ (1 - p(\Omega_2|\omega_A, t_{p4})) \rangle, \\ P_{01e} &= M_{01}\langle (1 - p(\Omega_2|\omega_A, t_{p2})) \ p(\Omega_2|\omega_A, t_{p4}) \rangle, \\ P_{01f} &= M_{01}\langle p(\Omega_2|\omega_A, t_{p2}) \ p(\Omega_2|\omega_A, t_{p4}) \rangle \end{aligned}$$

If the echo-forming MW pulses invert the partner spin in the pair with the probability 1, i.e., $p(\Omega_2|\omega_A, t_{p2}) = 1$, $p(\Omega_2|\omega_A, t_{p4}) = 1$, then the signal (Eq. (9)) is reduced to the well-known result $V_{01}(\tau_1, \tau_2) = \langle m_{1y} \rangle \cos(D(\tau_1 + \tau_2))$ [1–4]. This echo signal at $t = 2\tau_1 + 2\tau_2$ is produced by the recovery of the echo signal at $t = 2\tau_1$ due to the third refocusing MW pulse at $t = 2\tau_1 + \tau_2$. Note that the common factor M_{01} in the case of the primary echo signal without the pump MW pulse [Eq. (9)] is larger than the common factor M_1 in the case of the PELDOR signal [Eq. (8)]. This fact should be kept in mind when the PELDOR signal is normalized using the echo signal without the pump MW pulse as a reference signal.

The form of the PELDOR signal [Eq. (8)] becomes rather simple when the EPR spectra of two partners in the pair do not overlap. In this case only one spin of the pair, say R_1, contributes to the observable. Suppose that the EPR spectra of partner spins are well separated and the following assumptions are justified. The ω_A frequency MW pulses excite only R_1 spins, so that $p(\Omega_2|\omega_A, t_{p2}) = 0$ and $p(\Omega_2|\omega_A, t_{p4}) = 0$ while the ω_B frequency MW pulse excites only R_2 spins, so that $p(\Omega_1|\omega_B, t_{p3}) = 0$. Under these conditions, the PELDOR signal (8) is reduced to the result well known in the current theory (see Eq. (1)).

$$V(T, \tau_1, \tau_2) = \langle m_{1y} p(\Omega_1 | \omega_A, t_{p2}) \, p(\Omega_1 | \omega_A, t_{p4}) \rangle$$
$$\times \{ 1 - \langle p(\Omega_2 | \omega_B, t_{p3}) \rangle + \langle p(\Omega_2 | \omega_B, t_{p3}) \rangle \mathbf{cos}(\mathbf{D}(\tau_1 - \mathbf{T})) \} \quad (10)$$

Only one oscillating term appears in Eq. (10). In the general case of the paramagnetic particles in pairs with overlapping EPR spectra [Eq. (8)], the PELDOR signal contains six additional oscillating terms. All oscillating terms independent of the features of overlapping EPR spectra have the same frequency equal to the dipolar interaction parameter D. Amplitudes of these oscillating terms have the first-, second-, and third-order contributions over the probability of the inversion of R_1 and R_2 spins by the MW pulses. Keeping only the first-order terms one obtains from Eqs. (6) and (8).

$$V_{11}(T, \tau_1, \tau_2) = \boldsymbol{P_{11a}} + P_{11b}\cos(D\tau_1) + \boldsymbol{P_{11c}}\mathbf{cos}(\mathbf{D}(\tau_1 - \mathbf{T})) + P_{11e}\cos(D\tau_2), \quad (11)$$

where

$$\begin{aligned}
P_{11a} &= M_1 \langle (1 - p(\Omega_2 | \omega_A, t_{p2}) - p(\Omega_2 | \omega_B, t_{p3}) - p(\Omega_2 | \omega_A, t_{p4})) \rangle, \\
P_{11b} &= M_1 \langle p(\Omega_2 | \omega_A, t_{p2}) \rangle, \\
P_{11c} &= M_1 \langle p(\Omega_2 | \omega_B, t_{p3}) \rangle, \\
P_{11e} &= M_1 \langle p(\Omega_2 | \omega_A, t_{p4}) \rangle
\end{aligned} \quad (12)$$

Note that for the similar paramagnetic centers in pairs, e.g., when both partners are stable nitroxide radicals, the amplitudes of the three oscillating terms in Eq. (11) given by Eq. (12) are of comparable values (see Table 2).

Equation (12) show that the PELDOR signal contains two additional oscillating terms compared to the signal described in the current PELDOR theory, namely, P_{11b} $\cos(D\tau_1) + P_{11e} \cos(D\tau_2)$. These new terms originate from the fact that the echo-forming MW pulses can invert the partner spin in a pair if the EPR spectra of the partners in a pair overlap. Equation (12) show explicitly that these new terms are proportional to the probabilities $\langle p(\Omega_2 | \omega_A, t_{p2}) \rangle$ and $\langle p(\Omega_2 | \omega_A, t_{p4}) \rangle$ of the partner spin inversion by the second and fourth echo-forming MW pulses, respectively. It is worth to note that there is no contribution to the PELDOR signal described by the term like $\boldsymbol{P_{11c}}\mathbf{cos}(\mathbf{D}(\tau_1 - \mathbf{T}))$ if either the second or the fourth echo-forming MW pulse inverts the partner spin in a pair since for this case $P_{1c} = M_1(1 - p(\Omega_2 | \omega_A, t_{p2}))$ $p(\Omega_2 | \omega_B, t_{p3}) \, (1 - p(\Omega_2 | \omega_A, t_{p4})) = 0$.

Thus, Eqs. (11) and (12) describe the first-order effect of the EPR spectra overlapping on the four-pulse ELDOR signal. Equations (6) and (8) describe both effects: overlapping the EPR spectra of partners in pairs and possible overlapping of the excitation bands during the PELDOR experiment. According to the protocol of experiment (see Fig. 1), the second and fourth MW pulses have the same durations, i.e., $t_2 = t_4$, so that $\langle p(\Omega_2 | \omega_A, t_{p2}) \rangle = \langle p(\Omega_2 | \omega_A, t_{p4}) \rangle$. In this case, the amplitudes of the terms in the PELDOR signal [Eq. (8)] are determined by the following average probabilities of spin inversion:

$p_A \equiv \langle p(\Omega_2 | \omega_A, t_{p2}) \rangle$, $p_B \equiv \langle p(\Omega_2 | \omega_B, t_{p3}) \rangle$, $p_{AB} \equiv \langle p(\Omega_2 | \omega_A, t_{p2}) p(\Omega_2 | \omega_B, t_{p3}) \rangle$, $p_{AA} \equiv \langle p(\Omega_2 | \omega_A, t_{p2}) p(\Omega_2 | \omega_A, t_{p2}) \rangle$, $p_{ABA} \equiv \langle p(\Omega_2 | \omega_A, t_{p2}) p(\Omega_2 | \omega_B, t_{p3}) p(\Omega_2 | \omega_A, t_{p2}) \rangle$. The quantities p_{AB} and p_{ABA} characterize overlapping of the

Table 2 Values of p_A, p_B, p_{AA}, p_{AB}, p_{ABA} for the excitation patterns presented in Figs. 5a1–d1

Position of the excitation on the EPR spectrum	Simulation case $\omega_A - \omega_B > \omega_{1A} + \omega_{1B}$	Expected as optimal ω_B situation	Simulation case $\omega_A - \omega_B \approx \omega_{1A} + \omega_{1B}$	Simulation case $\omega_A = \omega_B$
ω_A ($\times 10^9$ s^{-1})	212.6	212.6	212.6	212.6
B_A (G)	12073.5	12073.5	12073.5	12073.5
ω_B ($\times 10^9$ rad s^{-1})	212.0	212.25	212.5	212.6
B_B (G)	12,040	12,054	12,068	12073.5
$p(\omega_A)$	0.1	0.1	0.1	0.1
$p(\omega_B)$	0.04	0.11	0.071	0.064
$p(\omega_A, \omega_A)$	0.054	0.054	0.054	0.054
$p(\omega_A, \omega_B)$	0.00058	0.0032	0.011	0.038
$p(\omega_A, \omega_A, \omega_B)$	0.000088	0.00035	0.0044	0.029

Rabi frequencies were chosen as $\omega_{1A} = 69.4 \times 10^6$ rad/s ($B_{1A} = 3.94$ G, the amplitude of the ω_A frequency MW pulses at $t = \tau_1$ (the second pulse), $t = 2\tau_1 + \tau_2$ (the fourth pulse, see Fig. 1), and for the pump MW pulse (the third pulse, see Fig. 1) $\omega_{1B} = 36.1 \times 10^6$ rad s^{-1}, $B_{1B} = 2.04$ G

excitation bands of the echo-forming and pump MW pulses. Using these notations, the PELDOR signal amplitudes P (Eq. (6)) can be written as

$$
\begin{aligned}
P_{1a} &= M_1(1 - 2p_A - p_B + p_{AA} + 2p_{AB} - p_{ABA}), \\
P_{1b} &= M_1(p_A - p_{AA} - p_{AB} + p_{ABA}), \\
P_{1c} &= M_1(p_B - 2p_{AB} + p_{ABA}), \\
P_{1d} &= M_1(p_{AB} - p_{ABA}), \\
P_{1e} &= M_1(p_A - p_{AA} - p_{AB} + p_{ABA}), \\
P_{1f} &= M_1(p_{AA} - p_{ABA}), \\
P_{1g} &= M_1(p_{AB} - p_{ABA}), \\
P_{1h} &= M_1 p_{ABA}
\end{aligned}
\tag{13}
$$

Due to the overlapping of the excitation bands, there appear three new oscillating terms in the PELDOR signal: $M_1((p_{AB} - p_{ABA})\ (\cos(DT) + \cos(D(\tau_1 + \tau_2 - T))) + p_{ABA}\ \cos(D(\tau_2 - T)))$. The quantities $p_A < 1$, $p_B < 1$ can be treated as relatively small first-order quantities. Then quantities p_{AA}, p_{AB} can be treated as the second-order and p_{ABA} as the third-order quantities. Thus, the overlapping of the excitation bands leads to the appearance of the second-order terms over the spin inversion probabilities. Note that in the current PELDOR theory, the observable [Eq. (1)] is characterized by the first-order parameter p_B, which is the probability of the spin inversion by the pump MW pulse. Below, we illustrate possible contributions of the terms which appear due to overlapping of the EPR spectra and overlapping of the excitation bands using the numerical calculations of the four-pulse ELDOR signal.

According to Eq. (3), the dipolar frequency D depends on the distance r between spins in the pair and the angle θ between the vector **r** and the direction of the external magnetic field. In the case of disordered systems, there is a random

distribution of orientations of the vector **r**, which connects the spin labels in the pair. Therefore, the contribution of the intra-pair interaction given by Eqs. (8)–(11) should be averaged over the random distribution of the polar angle θ. In addition, there can be the distribution $f(r)$ of the distance r between partners in pairs; therefore, Eqs. (8)–(11) should be averaged over this distribution as well. Thus, the observables [Eqs. (8–11)] are the result of the interference of the contributions oscillating with different frequencies D. This interference is described as average cosines.

$$\langle \cos Dt \rangle = \frac{1}{2} \int \cos\big(D_0\big(1 - 3\cos^2\theta\big)t\big) \sin\theta \, d\theta, \tag{14}$$

$$D_0 = \frac{g_A g_B \beta^2}{r^3},$$

The features of the average cosine [Eq. (14)] were discussed and presented in many publications and monographs (see, e.g., [29]). A recent review of this subject is given in Ref. [15]. Figure 2 illustrates the characteristic features of the average cosine [Eq. (14)]. There is a sharp decay at the early stage where the function drops down. Then it oscillates with the frequency close to the characteristic dipolar frequency D_0, which corresponds to the equatorial position of the vector **r** with respect to the direction of the external magnetic field.

The average cosine Eq. (14) can be presented in terms of Fresnel integrals [13]

$$\langle \cos Dt \rangle = \frac{\cos\frac{\pi y}{6}\, \text{FresnelC}\big(\sqrt{y}\big) + \text{FresnelS}\big(\sqrt{y}\big)\sin\frac{\pi y}{6}}{\sqrt{y}}, \tag{15}$$

where $y = 6D_0 t/\pi$. Equation (15) has an asymptotic value at $D_0 t \gg 1$

$$\langle \cos Dt \rangle \rightarrow \sqrt{\frac{\pi}{12 D_0 t}} \cos\Big(D_0 t - \frac{\pi}{4}\Big). \tag{16}$$

Asymptotically, the oscillation frequency tends to the singular frequency D_0.

In a PELDOR experiment, the signal is detected as a function of T. It is seen from Eq. (8) that there are terms independent of T, the term of the $\cos(DT)$ type and the terms of the $\cos(D(t-T))$ type, where $t = \tau_1$, or $t = \tau_2$, or $t = \tau_1 + \tau_2$. The average cosine $<\cos(D(t-T))>$ has a maximum at $T = t$ (see Fig. 3).

3 Results of Numerical Simulations of the Peldor Signal for Model Situations

We simulated numerically the four-pulse ELDOR signal [Eq. (8)]. For numerical simulations of the spin inversion probabilities, we used the EPR spectrum of the biradical containing 1-oxyl-2,2,5,5-tetramethylpyrroline-3-yl spin labels (Fig. 4). The EPR and the three-pulse ELDOR spectra of this biradical were experimentally studied in [15]. Note that we did not take into account any orientation selectivity effects in our model calculations below. So our calculations can serve only as an illustration of possible effects of overlapping of the EPR spectra and the excitation bands on the PELDOR signal.
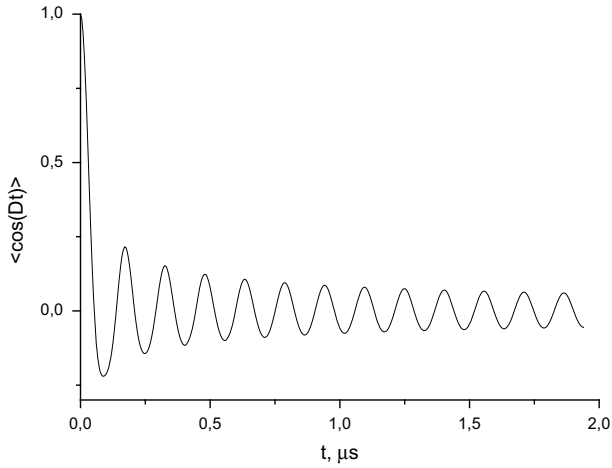
Fig. 2 Average cosine $<\cos(Dt)>$ calculated for $r = 2$ nm. The oscillation period is close to $T_0 = 2\pi/D_0 = 162.15$ ns
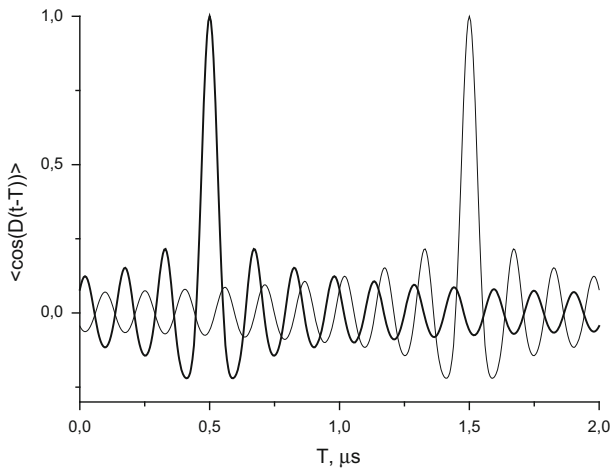

Fig. 3 Average cosines $<\cos(D(\tau_1 - T))>$ ($\tau_1 = 500$ ns, *thick curve*) and $<\cos(D(\tau_2 - T))>$ ($\tau_2 = 1,500$ ns, *thin curve*) calculated for $r = 2$ nm, $\tau_1 + \tau_2 = 2,000$ ns. Maxima occur at $T = \tau_1$ and $T = \tau_2$, respectively
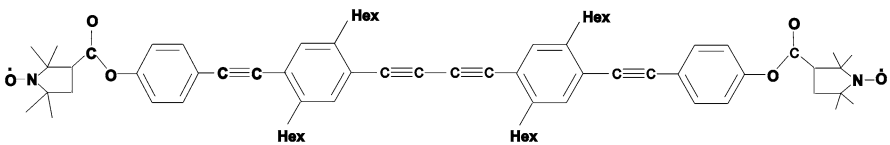

Fig. 4 Scheme of the biradical containing 1-oxyl-2,2,5,5-tetramethylpyrroline-3-yl spin labels

In this biradical spin centers are identical so that their EPR spectra coincide. We simulated the PELDOR signal for several values of the pump MW pulse frequency ω_B, while the frequency ω_A was kept constant, $\omega_A = 212.6 \times 10^9$ rad/s (the magnetic field of 12073.5 G). For comparison, we simulated simultaneously the PELDOR signal using the current theory Eq. (1), which does not take into account the overlapping of the EPR spectra of the two radical centers in the biradical. The results of these numerical simulations are presented in Fig. 5a–d. Note that in the case shown in Fig. 5b, the frequency ω_B is the EPR frequency at the most intense EPR signal so that this frequency is optimal for the PELDOR effect for the model situation. The simulations are done for the four values of the pump MW pulse frequency ω_B: far removed from the frequency ω_A (a1–a3), optimal frequency (b1–b3), close to ω_A (c1–c3), and equal to ω_A (d1–d3) frequencies. Parameters used during these simulations are given in Table 2. For this biradical, the inter-radical distance is 3.7 nm [15]. In this paper, we used the secular approximation for the dipole–dipole interaction in pairs. This approximation fails when the resonance frequencies of the partner spins in pairs are close which occurs definitely when the EPR spectra of the partners in pairs overlap. In this case, in principle, one has to take into account the pseudo-secular terms of dipole–dipole interaction when calculating the PELDOR signal. This was first pointed out for the case of coinciding frequencies in [30]. We plan to investigate this item quantitatively in the future work.

Parameters p which characterize the probabilities of the spin inversion scenarios were calculated numerically using Eqs. (4) and (7) and the spectrum of the 1-oxyl-2,2,5,5-tetramethylpyrroline-3-yl spin label. To visualize the EPR spectrum excitation bands, we presented on Fig. 5a1–d1 the EPR spectrum and the probability of the spin inversion (the excitation bands) by the corresponding MW pulses with the frequencies ω_A and ω_B.

The numerical data show that the values of p_{AB} and p_{ABA} are less than 0.01 and 0.0044 if $|\omega_A - \omega_B| \geq \omega_{1A} + \omega_{1B}$ and they can be neglected (see Table 2). Otherwise, all terms containing p_A, p_B, p_{AA}, p_{AB}, p_{ABA} give, in principle, comparable contributions to the PELDOR signal (see last column in Table 2).

Figure 5a–c support the expectation that under the condition $|\omega_A - \omega_B| \geq \omega_{1A} + \omega_{1B}$, the term $P_{1c} \cos(D(\tau_1 - T))$ gives the major contribution to the T dependence of the PELDOR signal [Eq. (8)]. Indeed, one can see in Fig. 5a2–c2 that the PELDOR signal has the maximum at $T = \tau_1$. However, the situation changes considerably when $|\omega_A - \omega_B| < \omega_{1A} + \omega_{1B}$. For example, when $\omega_A = \omega_B$ (see Fig. 5d), the pronounced maximum of the PELDOR signal occurs not at $T = \tau_1$, but at $T = \tau_2$. It is worth to note that within the current four-pulse ELDOR theory [Eq. (1)] the most pronounced maximum of the PELDOR signal is always expected at $T = \tau_1$. Note that the situation presented in Fig. 5b is optimal for the experiment since in this case the pump MW frequency ω_B corresponds to the maximum of the EPR intensity (see Fig. 5a1–d1) so that one expects the maximum of the PELDOR effect.

An important issue of the theory developed in this work concerns the value of the PELDOR signal amplitude when the time T is varied. Figure 5a2–b2 shows that the current theory overestimates the PELDOR signal amplitude up to 15–25 % when the excitation bands do not overlap essentially (compare the amplitudes of the thick
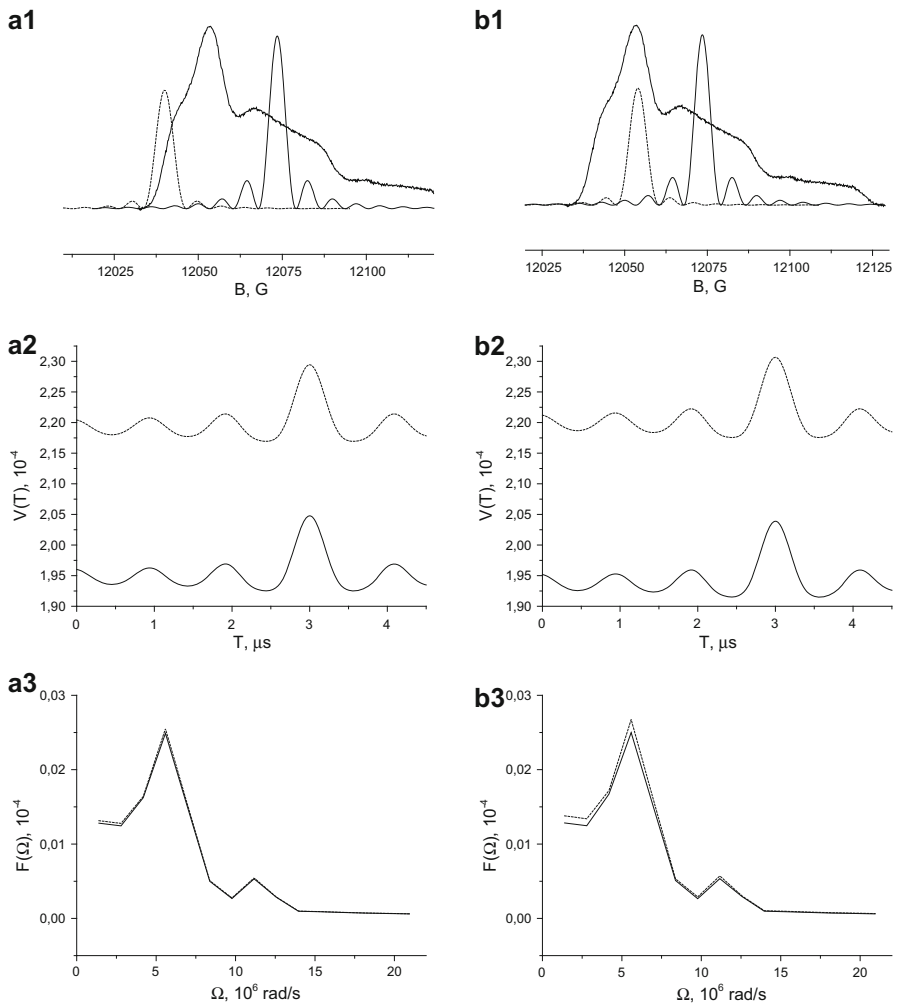
Fig. 5 EPR spectrum and excitation bands (**a1–d1**), dependence of the PELDOR signals on time T (**a2–d2**, *thick curves* are obtained using Eq. (8) and *dashed curves* obtained using Eq. (1) and the power Fourier transforms (**a3–d3**) of the PELDOR signals (**a2–d2**), respectively. These simulations were done assuming that $\tau_1 = 3 \times 10^{-6}$ s, $\tau_2 = 1.5 \times 10^{-6}$ s

and dashed curves at $T = 0$ in Fig. 5a2–b2). This 15–25 % decrease in the PELDOR signal amplitude is mainly due to overlapping of the EPR spectra of the partner spins in pairs. According to Eqs. (11) and (12), the relative contributions of terms $\cos(D\tau_1)$ and $\cos(D\tau_2)$ is determined by the probability of the spin inversion by the echo-forming pulses p_A which is 0.1 in the simulations (see Table 2). Alongside with the reduction of the PELDOR signal amplitude pointed out above, there is also the decrease in the modulation depth. For example in Fig. 5c2, the modulation depth predicted by the current theory (see dashed curve in Fig. 5c2) is about 1.5 times larger than that predicted by the theory developed in this work (see
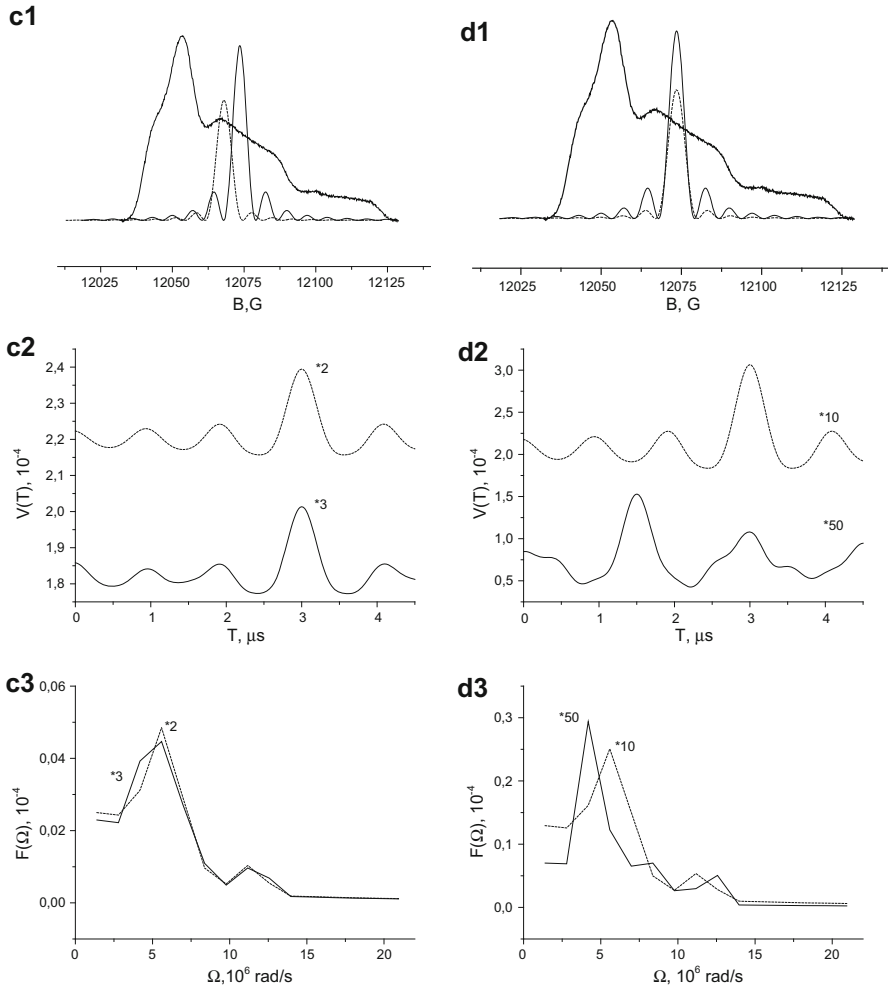
Fig. 5 continued

thick curve in Fig. 5c2). Note that the decrease of the modulation depth in the present theory arises as a result of the destructive interference of four $\cos(DT + \varphi)$ terms with $\varphi = 0$, $-D\tau_1$, $-D\tau_2$, $-D(\tau_1 + \tau_2)$ [see Eq. (8)]. When the excitation bands of the echo-forming and pump pulses coincide, the decrease in the PELDOR signal amplitude and the modulation depth becomes important. For example, the PELDOR signal amplitude and the modulation depth according to the present theory [Eq. (8)] is an order of magnitude less than that according to the current theory [Eq. (1)] if $\omega_A = \omega_B$ (see Fig. 5d).

Another issue of the present theory concerns the frequencies of the PELDOR signal oscillations. When $|\omega_A - \omega_B| < \omega_{1A} + \omega_{1B}$, the T dependence of the PELDOR signal can manifest "oscillations" with frequencies different from the characteristic dipolar frequency D (see Figs. 5c3, 3d). In fact, these additional frequencies are
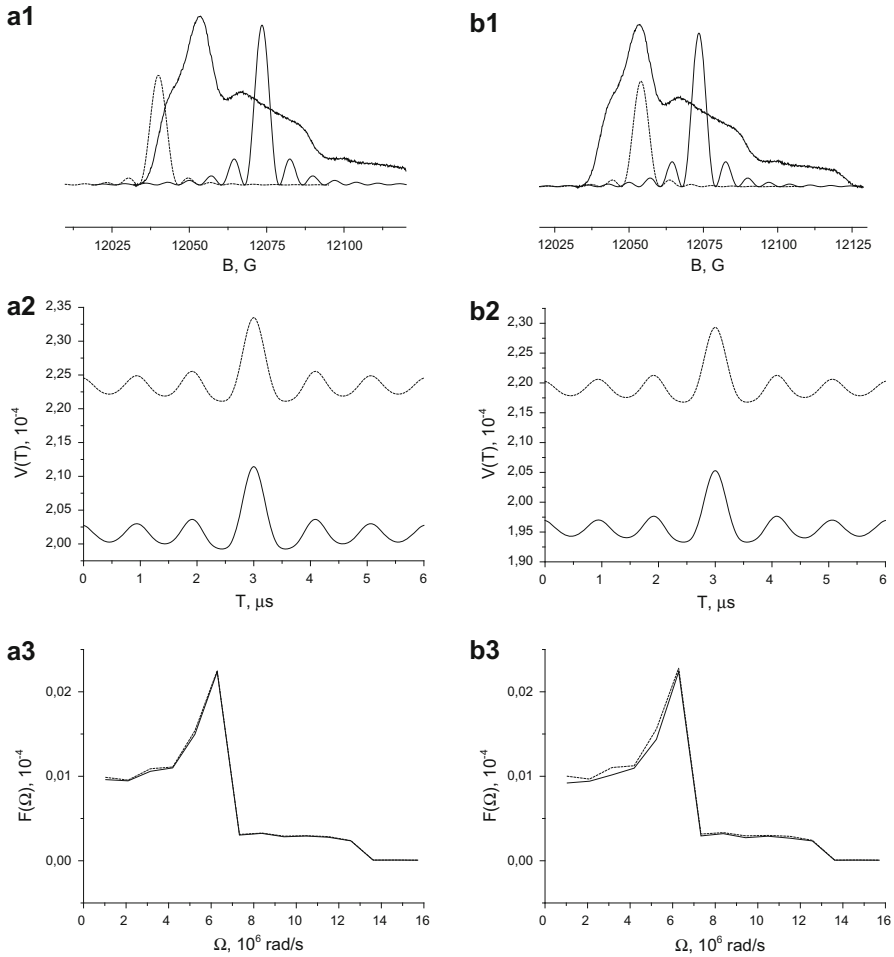
a1

b1

a2

b2

a3

b3

Fig. 6 EPR spectrum and excitation bands (**a1–d1**), dependence of the PELDOR signals on time T (**a2–d2**, *thick curves* are obtained using Eq. (8) and *dashed curves* obtained using Eq. (1) and the power Fourier transforms (**a3–d3**) of the PELDOR signals (**a2–d2**), respectively. Parameters used during these simulations are the same as in Fig. 5 except for $\tau_1 = \tau_2 = 3 \times 10^{-6}$ s

artifacts. The PELDOR signal contains several T-dependent terms: $P_{1d}\cos(DT) + \boldsymbol{P_{1c}\cos(D(\tau_1 - T))} + P_{1h}\cos(D(\tau_2 - T) + P_{1g}\cos(D(\tau_1 + \tau_2 - T)$ (see Eq. (8)). Each term oscillates with the same frequency D but these terms exhibit maxima at $T = 0$, $T = \tau_1$, $T = \tau_2$, $T = \tau_1 + \tau_2$, respectively. Thus, the Fourier transformation of the PELDOR signal can reveal additional "harmonics" associated with these local maxima in the PELDOR signal despite the fact that all PELDOR signal terms oscillate with the characteristic dipolar frequency D. To illustrate the effect of τ_1 and τ_2 on the appearance of these artifact "modulation" frequencies, we present simulations (Fig. 6) for the case $\tau_1 = \tau_2 = 3 \times 10^{-6}$ s, while all other parameters are the same as in Fig. 5.
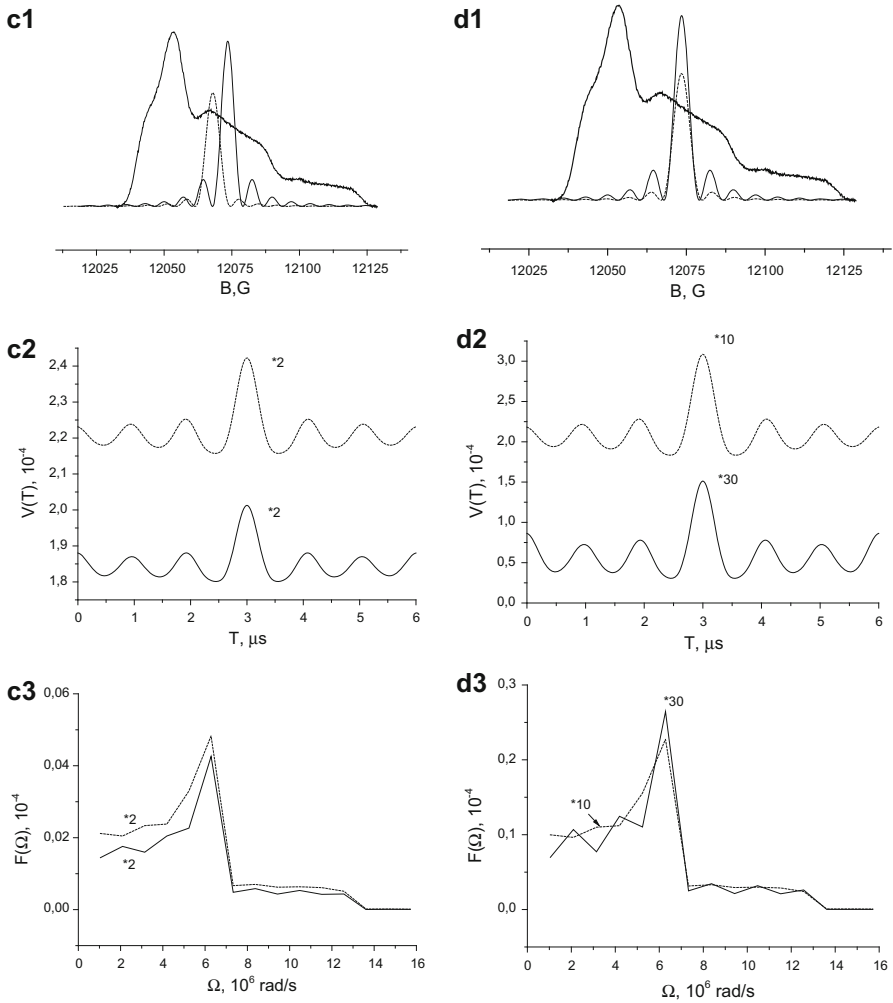
Fig. 6 continued

The comparison of the curves presented in Figs. 5 and 6 shows that the Fourier transformation of the PELDOR signal changes when τ_1 and τ_2 are varied if the frequencies ω_A and ω_B are close so that the excitation bands overlap.

4 Conclusions

The theory of the four-pulse ELDOR of an ensemble of the pairs of the ½ spin paramagnetic particles was extended to the general case when the EPR spectra of the partners in the pair overlap or even coincide. We also investigated theoretically the effect of overlapping of the observer and pump excitation bands on the four-

pulse ELDOR signal. Overlapping of the EPR spectra of the partners in pairs and overlapping of the excitation bands lead to additional terms of different types. Overlapping of the EPR spectra is responsible for the contributions to the PELDOR signal, which does not depend on the time T when the pump pulse is applied. So these contributions affect mainly the PELDOR signal amplitude and not the frequency of the PELDOR signal modulation. The PELDOR signal amplitude may be of minor importance when studying pairs of spin labels. But it is of major importance when studying a number of spin labels, the architecture of spin label arrangement, when groups of spins are investigated using PELDOR (e.g., see discussion of this item in [15]). Due to overlapping of the excitation bands, the depth of the PELDOR signal modulation decreases. This effect originates from the destructive interference of several contributions which have different initial phases. Moreover, due to overlapping of the excitation bands, the artifact frequencies of the PELDOR signal "oscillations" can be observed. These additional artifact frequencies can be specified by varying the time intervals τ_1 and τ_2 used in the four-pulse ELDOR experiment.

The results obtained in this work for pairs of spin labels can be extended to groups of spins. In [15] for the case of the three-pulse ELDOR, we described in detail how this extension can be done.

References

1. W.B. Mims, in *Electron Paramagnetic Resonance*, ed. by S. Geschwind (Plenum Press, New York, 1972), pp. 263–351
2. K.M. Salikhov, A.G. Semenov, Yu.D. Tsvetkov, *Electron Spin Echoes and Their Applications* (Nauka, Novosibirsk, 1976) (in Russian)
3. K.M. Salikhov, Yu.D. Tsvetkov, in *Time-Domain ESR Spectroscopy*, ed. by L. Kevan, R. Schwartz (Wiley, New York, 1979)
4. A.M. Raitsimring, K.M. Salikhov, Bull. Magn. Reson. **7**, 184–195 (1985)
5. V.V. Kurshev, A.M. Raitsimring, T. Ichikawa, J. Phys. Chem. **95**, 3564–3568 (1991)
6. V.F. Yudanov, K.M. Salikhov, G.M. Zhidomirov, Theor. Eksper. Khim. **5**, 663–668 (1969)
7. G.M. Zhidomirov, K.M. Salikhov, ZhETP **56**, 1933–1939 (1969)
8. L.V. Kulik, S.A. Dzuba, L.A. Grigoryev, Yu.D. Tsvetkov, Chem. Phys. Lett. **343**, 315–324 (2001)
9. A.D. Milov, K.M. Salikhov, M.D. Schirov, Fiz. Tverd. Tela **23**, 975–982 (1981)
10. A.D. Milov, A.G. Maryasov, Yu.D. Tsvetkov, Appl. Magn. Reson. **15**, 107–143 (1998)
11. A.G. Maryasov, Yu.D. Tsvetkov, J. Raap, Appl. Magn. Reson. **14**, 101–114 (1998)
12. G. Jeschke, Ye. Polyhach, Phys. Chem. Chem. Phys. **9**, 1895–1910 (2007)
13. Yu.D. Tsvetkov, A.D. Milov, A.G. Maryasov, Usp. Khim. **77**, 487–520 (2008)
14. G. Jeschke, Ann. Rev. Phys. Chem. **63**, 419–446 (2012)
15. K.M. Salikhov, I.T. Khairuzhdinov, R.B. Zaripov, Appl. Magn. Reson. **45**, 573–620 (2014)
16. R.E. Martin, M. Pannier, F. Diederich, V. Gramlich, M. Hubrich, H.W. Spiess, Angew. Chem. Int. Ed. Engl. **37**, 2834–2837 (1998)
17. H.W. Spiess, J. Magn. Reson. **213**, 326–328 (2011)
18. M. Pannier, S. Veit, A. Godt, G. Jeschke, H.W. Spiess, J. Magn. Reson. **142**, 331–340 (2000)
19. R.G. Larsen, D.J. Singel, J. Chem. Phys. **98**, 5134–5146 (1993)
20. G. Jeschke, A. Koch, U. Jonas, A. Godt, J. Magn. Reson. **155**, 72 (2001)

21. G. Jeschke, M. Sajid, M. Schulte, A. Godt, Phys. Chem. Chem. Phys. **11**, 6580–6591 (2009)
22. A.D. Milov, Yu.D. Tsvetkov, J. Raap, Appl. Magn. Reson. **19**, 215–226 (2000)
23. A.D. Milov, B.D. Naumov, YuD Tsvetkov, Appl. Magn. Reson. **26**, 587–599 (2004)
24. D. Margraf, P. Cekan, T.F. Prisner, S.Th. Sigurdsson, O. Schiemann, Phys. Chem. Chem. Phys. **11**, 6708–6714 (2009)
25. K. Moebius, A. Savitsky, *High-Field EPR Spectroscopy on Proteins and Their Model Systems* (RSC Publishing, Cambridge, 2009)
26. A.F. Bedilo, A.G. Maryasov, J. Magn. Reson. **A116**, 87–96 (1995)
27. A. Godt, M. Schulte, H. Zimmermann, G. Jeschke, Chem. Phys. Phys. Chem. **45**, 7560–7564 (2006)
28. Y. Polyhach, E. Bordignon, R. Tschaggelar, S. Gandra, A. Godt, G. Jeschke, Chem. Phys. Phys. Chem. **14**, 10762–10773 (2012)
29. A. Abragam, *The Principles of Nuclear Magnetism* (Clarendon Press, Oxford, 1961)
30. G. Jeschke, M. Pannier, A. Godt, H.W. Spiess, Chem. Phys. Lett. **331**, 243–252 (2000)